The University of Michigan

UMBmark —

A Method for Measuring, Comparing, and Correcting Dead-reckoning Errors in Mobile Robots

by

J. Borenstein[1] and L. Feng[2]

with the help of

Professors D. K. Wehe and Y. Koren

and Grad. Students Z. Fan, B. Holt, and B. Costanza

December 1994

Copies of this report are available from the University of Michigan as: Technical Report UM-MEAM-94-22

Prepared by the University of Michigan
For the Oak Ridge National Lab (ORNL) D&D Program
and the
United States Department of Energy's
Robotics Technology Development Program
Within the Environmental Restoration, Decontamination and Dismantlement Project

1) Dr. Johann Borenstein	2) Dr. Liqiang Feng
The University of Michigan	The University of Michigan
Department of Mechanical	Department of Mechanical
Engineering and Applied Mechanics	Engineering and Applied Mechanics
Mobile Robotics Laboratory	Mobile Robotics Laboratory
1101 Beal Avenue	1101 Beal Avenue
Ann Arbor, MI 48109	Ann Arbor, MI 48109
Ph.: (313) 763-1560	Ph.: (313) 936-9362
Fax: (313) 944-1113	Fax: (313) 763-1260
Email: Johannb@umich.edu	Email: Feng@engin.umich.edu

Please direct all inquiries to Johann Borenstein

Executive Summary

Dead-reckoning is the most widely used method for determining the momentary position of a mobile robot. In most practical applications dead-reckoning provides easily accessible real-time positioning information in-between periodic absolute position measurements. The frequency at which the (usually costly and/or time-consuming) absolute measurements must be performed depends to a large degree on the accuracy of the dead-reckoning system.

This report introduces a method for measuring dead-reckoning errors in mobile robots, and for expressing these errors quantitatively. When measuring dead-reckoning errors, one must distinguish between (1) *systematic* errors, which are caused by kinematic imperfections of the mobile robot (for example, unequal wheel-diameters), and (2) *non-systematic* errors, which may be caused by wheel-slippage or irregularities of the floor. *Systematic* errors are a property of the robot itself, and they stay almost constant over prolonged periods of time, while non-systematic errors are a function of the properties of the floor.

Our method, called the *University of Michigan Benchmark test* (UMBmark), is especially designed to uncover certain *systematic* errors that are likely to compensate for each other (and thus, remain undetected) in less rigorous tests. This report explains the rationale for the carefully designed UMBmark procedure and explains the procedure in detail. Experimental test results from different mobile robots are presented and discussed. Our report also proposes a method called *extended UMBmark* for measuring non-systematic errors. Although the measurement of non-systematic errors is less useful because it depends strongly on the floor characteristics, one can use the *extended UMBmark* test for comparison of different robots under similar conditions. This report presents experimental results from six different vehicles tested for their susceptibility to *non-systematic* error by means of the *extended UMBmark* test. With the quantitative benchmark test proposed here, researchers will be able to compare the dead-reckoning accuracy of different robots, or they can measure and tune the performance of a single robot.

Perhaps the foremost contribution of the work described here is a unique and innovative method for the calibration of mobile robots. This method is called *UMBmark calibration* because it is based on measurements from the UMBmark test. Performing an occasional calibration as proposed here will increase the robot's dead-reckoning accuracy and reduce operation cost because an accurate mobile robot requires fewer absolute positioning updates. Many manufacturers or end-users calibrate their robots, usually in a time-consuming and non-systematic trial and error approach. By contrast, the *UMBmark calibration* is systematic and provides near-optimal results. Our procedure for measuring and correcting systematic dead-reckoning errors can be performed easily and without complicated equipment. Furthermore, UMBmark lends itself readily for adaptation as an automated self-calibration procedure. Experimental results are presented that show a consistent improvement of at least one order of magnitude in dead-reckoning accuracy (with respect to systematic errors) for a mobile robot calibrated with the UMBmark calibration.

Table of Content

6. CORRECTION OF SYSTEMATIC DEAD-RECKONING ERRORS

One interesting aspect of the error distribution pattern in the UMBmark experiment (see Fig. 3.4, in Section 3.3, above) is the fact that one can analytically derive correction factors from the experimental results. Before we do so, let us first define two new error characteristics that are meaningful only in the context of the Bi-directional Square Path experiment. These characteristics, called Type A and Type B, represent dead-reckoning errors in orientation. Type A is defined as an orientation error that ***reduces (or increases)*** the total amount of rotation of the robot during the square path experiment in ***both cw and ccw direction***. By contrast, Type B is defined as an orientation error that ***reduces (or increases)*** the total amount of rotation of the robot during the square path experiment in **one direction**, but ***increases (or reduces)*** the amount of rotation when going in the ***other direction***. As examples consider Figures 6.1 and 6.2, further below. Figure 6.1 shows a case where the robot turns four times for a nominal amount of 90º per turn. However, because the actual wheelbase of the vehicle was larger than the nominal value, the vehicle actually turned only 85º in each corner of the square path. In the example of Fig. 6.1 the robot will actually turn only $\theta_{total} = 4\times85^{o} = 340^{o}$, instead of the desired $\theta_{nominal} = 360^{o}$. We observe that in ***both the cw and the ccw*** experiment the robot ends up turning ***less*** than the desired amount , i.e., $|\theta_{total,\ cw}| < |\theta_{nominal}|$ ***and*** $|\theta_{total,\ ccw}| < |\theta_{nominal}|$. Thus, the orientation error is of Type A. In Fig. 6.2 the trajectory of a robot with unequal wheel diameters is shown. This error expresses itself in a curved path that adds to the overall orientation at the end of the run in ccw direction, but it reduces the overall rotation in the ccw direction, i.e., $|\theta_{total,\ ccw}| > |\theta_{nominal}|$ ***but*** $|\theta_{total,\ cw}| < |\theta_{nominal}|$. Thus, the orientation error in Fig. 6.2 is of Type B.

In an actual run Type A and Type B errors will of course occur together. The problem is therefore how to distinguish and compute Type A and Type B errors from the measured final position errors of the robot in the Bi-directional Square Path experiment. We approach this problem by defining a simplified model for systematic dead-reckoning errors. This model assumes that

1. E_d and E_b are the dominant sources of systematic dead-reckoning errors.
2. An incorrect wheelbase (E_b) causes errors only during turning but not during straight line motion.
3. Unequal wheel diameters (E_d) cause errors only during straight line motion but not during turning. This assumption is substantiated in Appendix B.
4. E_b causes only Type A errors but not Type B errors.
5. E_d causes only Type B errors but not Type A errors.
6. Because of assumption #1, eliminating E_b eliminates the system's Type A error *almost* completely.
7. Because of assumption #1, eliminating E_d eliminates the system's Type B error *almost* completely.
8. Orientation errors are the main source of concern because once they are incurred they grow without bound into lateral position errors [Crowley, 1989; Feng et al., 1993].

Because of the close association between E_b and Type A errors and between E_d and Type B errors (according to assumptions #6 and #7) we will use the terms E_b and Type A, as well as the terms E_d and Type B, interchangeably.

6.1 Analysis of Type A and Type B Errors

Having defined a model, we will now analyze the characteristics of the UMBmark procedure with regard to that model. To simplify the mathematical treatment, we note that the following approximations are valid for small angles:

$$\begin{aligned} L\sin\gamma &\approx L\gamma \\ L\sin 2\gamma &\approx 2L\gamma \\ L\sin 3\gamma &\approx 3L\gamma \end{aligned} \qquad (6.1)$$

$$\begin{aligned} L\cos\gamma &\approx L \\ L\cos 2\gamma &\approx L \\ L\cos 3\gamma &\approx L \end{aligned} \qquad (6.2)$$

where
L - the length of each side of the square path.
γ - any incremental orientation error caused by either E_d or E_b, measured in [rad].

For simplicity, we assume that the starting position (x_0, y_0) of the robot is at (0,0). At first we will analyze and examine the contribution of Type A and Type B errors separately. Then, we will superimpose both errors to represent the actual conditions.

Figure 6.1 shows the contribution of Type A errors. We recall that according to assumptions #1 and #4 Type A errors are caused mostly by E_b. We also recall that Type A errors cause too much or too little turning at the corners of the square path. The (unknown) amount of erroneous rotation in each nominal 90° turn is denoted as α. Because of the approximations in Eqs. (6.1) and (6.2), α is measured in [rad].

a. For Type A errors in ccw direction:

$$x_1 = x_0 + L \qquad (6.3a)$$
$$y_1 = y_0 \qquad (6.3b)$$

$$x_2 = x_1 + L\sin\alpha \approx L + L\alpha \qquad (6.4a)$$
$$y_2 = y_1 + L\cos\alpha \approx L \qquad (6.4b)$$

$$x_3 = x_2 - L\cos 2\alpha \approx L\alpha \qquad (6.5a)$$
$$y_3 = y_2 + L\sin 2\alpha \approx L + 2L\alpha \qquad (6.5b)$$

$$x_4 = x_3 - L\sin 3\alpha \approx -2L\alpha \qquad (6.6a)$$
$$y_4 = y_3 - L\cos 3\alpha \approx 2L\alpha \qquad (6.6b)$$

b. For Type A errors in cw direction:

$$x_1 = x_0 + L \qquad (6.7a)$$
$$y_1 = y_0 \qquad (6.7b)$$

$$x_2 = x_1 + L\sin\alpha \approx L + L\alpha \qquad (6.8a)$$
$$y_2 = y_1 - L\cos\alpha \approx -L \qquad (6.8b)$$

$$x_3 = x_2 - L\cos 2\alpha \approx L\alpha \qquad (6.9a)$$
$$y_3 = y_2 - L\sin 2\alpha \approx -L - 2L\alpha \qquad (6.9b)$$

$$x_4 = x_3 - L\sin 3\alpha \approx -2L\alpha \qquad (6.10a)$$
$$y_4 = y_3 + L\cos 3\alpha \approx -2L\alpha \qquad (6.10b)$$

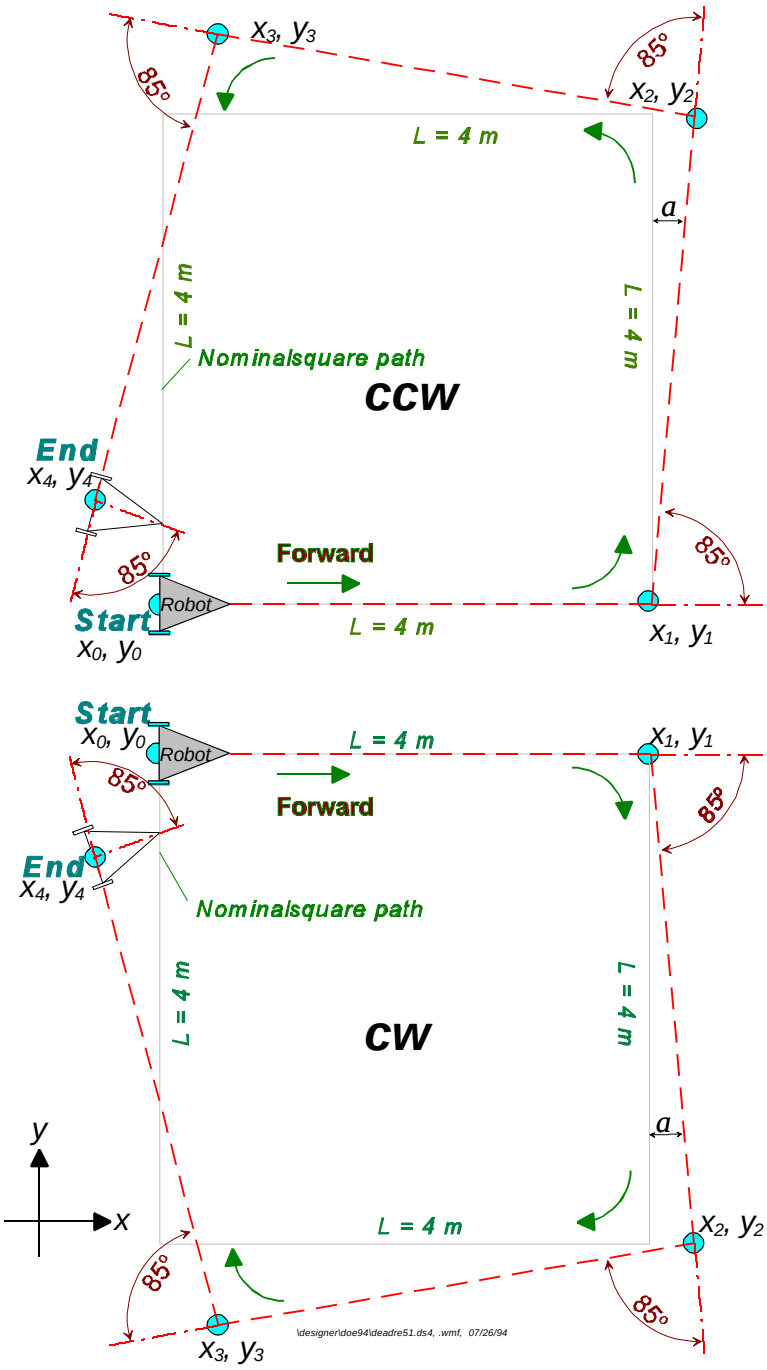

Figure 6.1: Type A errors in ccw and cw direction. Type A errors are caused almost exclusively by the wheelbase error E_b.

Figure 6.2 shows the contribution of Type B errors. We recall that according to our assumptions #1 and #5 Type B errors are caused mostly by the ratio between wheel diameters, E_d. We also recall that Type B errors cause a slightly curved path instead of a straight one during the four straight legs of the square path. Because of the curved motion, the robot will have gained an incremental orientation error, denoted β, at the end of each straight leg. Note that the auxiliary line c'_1, which connects the corner points of the actual path, has a slope of $\beta/2$ because it is parallel to the tangent to the midpoint of arc c_1. With respect to the unknown parameter β (in [rad]), we obtain:

a. For Type B errors in ccw direction:

$$x_1 = x_0 + L\cos(\beta/2) \approx L \quad (6.11a)$$
$$y_1 = y_0 + L\sin(\beta/2) \approx L\beta/2 \quad (6.11b)$$

$$x_2 = x_1 - L\sin(3\beta/2) \approx L - 3L\beta/2 \quad (6.12a)$$
$$y_2 = y_1 + L\cos(3\beta/2) \approx L\beta/2 + L \quad (6.12b)$$

$$x_3 = x_2 - L\cos(5\beta/2) \approx -3L\beta/2 \quad (6.13a)$$
$$y_3 = y_2 - L\sin(5\beta/2) \approx -2L\beta + L \quad (6.13b)$$

$$x_4 = x_3 + L\sin(7\beta/2) \approx 2L\beta \quad (6.14a)$$
$$y_4 = y_3 - L\cos(7\beta/2) \approx -2L\beta \quad (6.14b)$$

b. For Type B errors in cw direction:

$$x_1 = x_0 + L\cos(\beta/2) \approx L \quad (6.15a)$$
$$y_1 = y_0 + L\sin(\beta/2) \approx L\beta/2 \quad (6.15b)$$

$$x_2 = x_1 + L\sin(3\beta/2) \approx L + 3L\beta/2 \quad (6.16a)$$
$$y_2 = y_1 - L\cos(3\beta/2) \approx L\beta/2 - L \quad (6.16b)$$

$$x_3 = x_2 - L\cos(5\beta/2) \approx 3L\beta/2 \quad (6.17a)$$
$$y_3 = y_2 - L\sin(5\beta/2) \approx -L(2\beta + 1) \quad (6.17b)$$

$$x_4 = x_3 - L\sin(7\beta/2) \approx -2L\beta \quad (6.18a)$$
$$y_4 = y_3 + L\cos(7\beta/2) \approx -2L\beta \quad (6.18b)$$

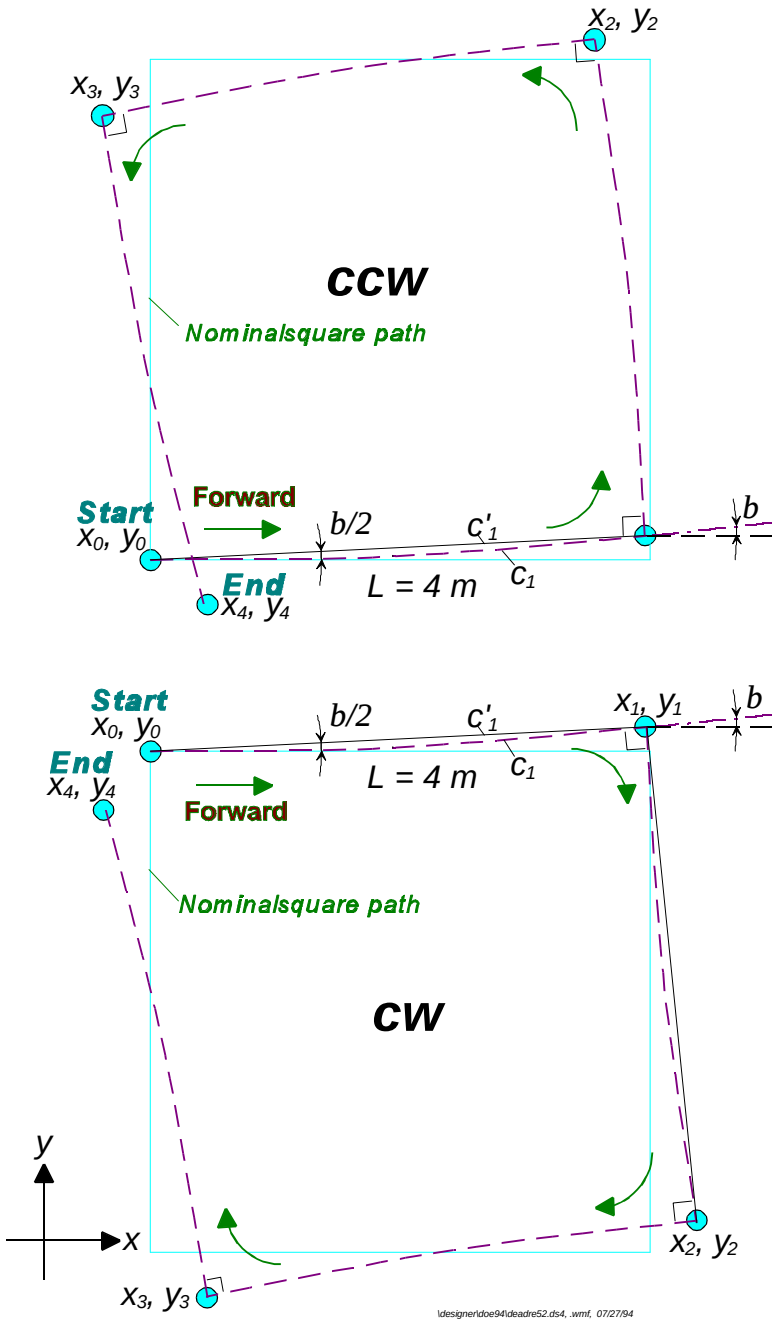

Figure 6.1: Type B errors in ccw and cw direction. Type B errors are caused almost exclusively by unequal wheel diameters (E_d).

Superimposing Type A and Type B errors for the cw experiment in x-direction yields

x_{cw}: $-2L\alpha - 2L\beta = -2L(\alpha + \beta) = x_{c.g.,cw}$ (6.19)

x_{ccw}: $-2L\alpha + 2L\beta = -2L(\alpha - \beta) = x_{c.g.,ccw}$ (6.20)

Subtracting (6.20) from (6.19) yields

$$-4L\beta = x_{c.g.,cw} - x_{c.g.,ccw} \quad (6.21)$$

or

$$\beta = \frac{x_{c.g.,cw} - x_{c.g.,ccw}}{-4L} \frac{(180^o)}{\pi} \quad (6.22a)$$

for β in degrees.

Comparing terms in y-direction yields a similar result

$$\beta = \frac{y_{c.g.,cw} + y_{c.g.,ccw}}{-4L} \frac{(180^o)}{\pi} \quad (6.22b)$$

Using simple geometric relations, the radius of curvature *R* of the curved path of Fig. 6.2 can be found from triangle ABM in Fig. 6.3.

$$R = \frac{L/2}{\sin(\beta/2)} \quad (6.23)$$

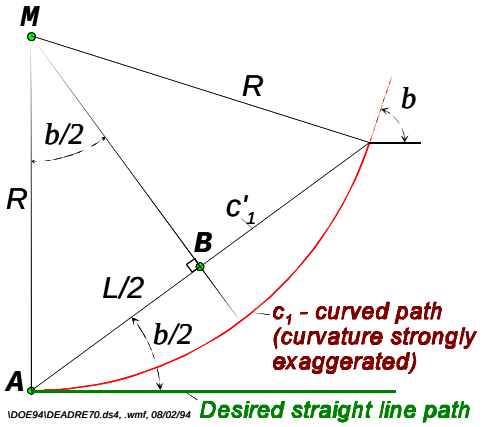

Figure 6.3: Geometric relations for finding the radius of curvature.

Once the radius *R* is computed, it is easy to determine the ratio between the two wheel diameters that caused the robot to travel on a curved, instead of a straight path (see Fig. 6.4):

$$E_d = \frac{D_R}{D_L} = \frac{R + b/2}{R - b/2} \quad (6.24)$$

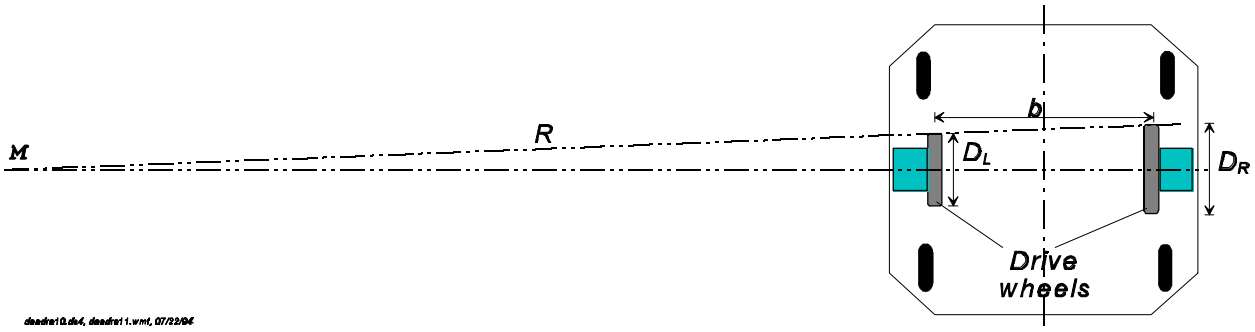

Figure 6.4: Unequal wheel diameters cause the robot to travel on a curved path of radius *R* (curvature is exaggerated for better illustration).

The ratio of Eq. (6.24) can be used to correct Type B errors as will be explained in Section 6.2.

Similarly, α can be found by adding Eq. (6.19) and Eq. (6.20)

$$-4L\alpha = x_{c.g.,cw} + x_{c.g.,ccw} \tag{6.25}$$

or

$$\alpha = \frac{x_{c.g.,cw} + x_{c.g.,ccw}}{-4L}\left(\frac{180^o}{\pi}\right) \tag{6.26a}$$

solves for α in [degrees].

Again, comparing terms in y-direction yields a similar result for α

$$\alpha = \frac{y_{c.g.,cw} - y_{c.g.,ccw}}{-4L}\ \frac{(180^o)}{\pi} \tag{6.26b}$$

We can now compute the wheelbase error E_b. Since the wheelbase b is directly proportional to the actual amount of rotation as shown by Eq. (2.4), we can use the proportion:

$$\frac{b_{actual}}{90^o} = \frac{b_{nominal}}{90^o - \alpha} \tag{6.27}$$

so that

$$b_{actual} = \frac{90^o}{90^o - \alpha}\ b_{nominal} \tag{6.28}$$

where, per definition of Eq. (2.8)

$$E_b = \frac{90^o}{90^o - \alpha} \tag{6.29}$$

6.2 Compensation for systematic dead-reckoning errors

Once we know the quantitative values of E_d and E_b, it is easy to compensate for these errors in software. The correction for the wheelbase error E_b is trivial: the wheelbase b is redefined in software according to Eq. (6.28). The correction for the unequal wheel diameters, E_d, is slightly more complex: After performing the UMBmark procedure, we know the *actual* wheel diameter ratio $E_d = D_R/D_L$ from Eq. (6.24). However, when applying a compensation factor, we must make sure not to change the *average* wheel diameter D_a, since one would then have to recalibrate that parameter. D_a will remain unchanged if we consider it as a constraint

$$D_a = (D_R + D_L)/2 \tag{6.30}$$

Solving Eqs. (6.24) and (6.30) as a set of two linear equations with two unknowns, D_R and D_L, yields

$$D_L = \frac{2}{E_d + 1} D_a \tag{6.31}$$

and

$$D_R = \frac{2}{(1/E_d) + 1} D_a \tag{6.32}$$

We can now define the two correction factors

$$c_L = \frac{2}{E_d + 1} \tag{6.33}$$

and

$$c_R = \frac{2}{(1/E_d) + 1} \tag{6.34}$$

which can be implemented in the dead-reckoning algorithm by rewriting Eq. (2.2) as

$$\Delta U_{L/R,\,I} = c_{L/R}\, c_m\, N_{L/R,\,I} \tag{6.35}$$

We have thus corrected both dominant systematic errors.

6.3 Correction of Systematic Errors

In this section we describe experiments that validate the above described method for correcting Type A and Type B errors by changing the effective wheelbase b and the effective wheel-diameter ratio D_R/D_L. The experiments were performed with a LabMate robot equipped with an onboard AMPRO 486/50 MHZ PC compatible single-board computer.

The robot was programmed for both a cw and a ccw 4×4 m square path. To avoid slippage, the robot was traveling slowly, at a speed of 0.2 m/s during the straight legs of the square path. At the end of each leg the robot came to a complete stop and rotated on-the-spot through 90°. This means that the robot made a fourth 90° turn after returning to its starting area. The linear speed of the two drive wheels during turning was approximately 0.2 m/s and -0.2 m/s. The robot started and stopped near an L-shaped corner and used a so-called "*sonar calibrator*" [Borenstein 1993] to determine its position and orientation relative to the L-shaped corner. We will refer to this as the *absolute* position. The sonar calibrator comprises three standard POLAROID ultrasonic sensors. Two sensors were facing the long side of the L-shaped corner, the third sensor faced the short side. The ultrasonic sensor system allowed measurement of the absolute position of the vehicle to within ±2 millimeters in the x and y directions, and to about ±0.4° in orientation.

At the beginning of each run a sonar measurement was taken to determine the starting position of the vehicle. The robot then traveled through the programmed path and returned to the L-shaped corner, where the *perceived* position (i.e., the position the vehicle "thought" it had, based on dead-reckoning) was recorded. Then, a second sonar measurement was taken to determine the *absolute* position. The difference between the absolute position and the perceived position is called the *return position error* ϵ; ϵ is defined by Eqs. (3.1), above.

The uncalibrated robot (i.e., D_R/D_L = 1.0000 and $b = b_{nominal}$ = 340.00 mm) made five cw trips and five ccw trips. As expected, the *return position errors* were clearly grouped in a cw cluster and a ccw cluster, as was shown in Fig. 5. For each of the two clusters the x and y components of the respective centers of gravity were computed according to Eq. (3.2). The resulting $x_{c.g.}$ and $y_{c.g.}$ were used to compute E_d according to Eqs. (6.22) - (6.24). Then, correction factors c_L and c_R were computed according to Eqs. (6.33) and (6.34) and introduced into the dead-reckoning program. Similarly the corrected wheelbase b_{new} was computed according to Eqs. (6.26) - (6.28)[2].

At this time the calibration procedure was complete. In order to verify the results we ran the UMBmark experiment for a second time, this time with the correction factors in place. Figure 6.5 shows the results of both the uncalibrated runs and the runs with the calibrated vehicle.

As explained in Section 3, Eqs. (3.2) and (3.3) were used to express the experimental results quantitatively as the *measure of dead-reckoning accuracy for systematic errors*, $E_{max,syst}$. In the example of Fig. 6.5, $E_{max,syst}$ was 317 mm before compensation and 21 mm after compensation. This represents a 15-fold improvement.

In order to assure that the experiment shown in Fig. 6.5 was not an isolated case, we performed another seven carefully monitored experiments. Table I lists the results from all eight experiments. We emphasize that Table I lists **all** experiments we ever made, it is not a selection of the best runs. We further emphasize that in each experiment we used all runs, without eliminating "outliers" (with the exception of four or five runs where the errors reported by the *sonar calibrator* were absurdly large, presumably due to a malfunctioning of the *sonar calibrator*).

The seemingly large fluctuations in improvement, especially among experiments #3, #4, and #5 (which all used the same correction factors) are due to the fact that the *centers of gravity* (c.g.s) for the runs after calibration are all very close to the origin (as seen in Fig. 6.5).

---

[2] Hoping to reduce the effect of non-systematic errors further, we actually computed E_d and E_b in two ways: (1) based on the values for $x_{c.g.}$, according to Eqs. (6.22a) and (6.26a); and (2) based on the values for $y_{c.g.}$, according to Eqs. (6.22b) and (6.26b). We then averaged $E_{d,x}$ and $E_{d,y}$, as well as $E_{b,x}$ and $E_{b,y}$. This measure may not be necessary in general, because the respective correction values (based on $x_{c.g.}$ or $y_{c.g.}$) differed by less than 1% in all cases.

Thus, the arbitrary spread of return position errors caused by non-systematic error sources has greater impact on the c.g.s. For example, the c.g. of Experiment 4 is only 17 mm (5/8") closer to the origin than the c.g. of Experiment #3 — a difference that is easily attributable to the arbitrary spread of non-systematic errors.

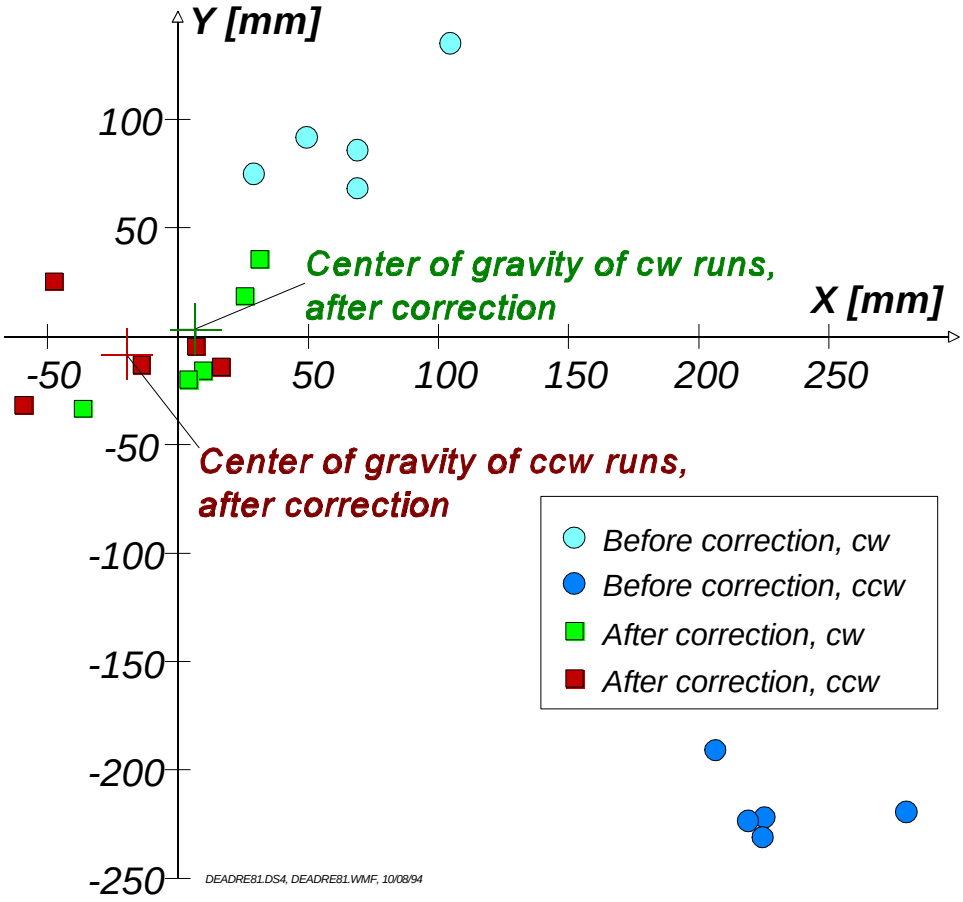

Figure 6.5: Position errors of a TRC LabMate after completing the UMBmark test (4 x 4 m).
Before calibration: b=340.00 mm, D_R/D_L = 1.00000
After calibration: b=336.17 mm, D_R/D_L = 1.00084

In principle, it is possible to achieve even better results by performing the compensation procedure for a second time, "on top of" the first compensation. This is so because a compensated robot can be treated as though it was a "new" uncompensated robot, but with different initial parameters. Using the *standard deviation* (σ) of the 5 runs in each direction it is easy to decide when a second compensation run will be beneficial. The standard deviation of the *return position errors* in the UMBmark test was about σ = 25 mm. The *Standard Error of the Mean* (SEM), defined as SEM = σ/sqrt(*n*), was 11.2 mm (*n* is the number of runs). As a rule-of-thumb sometimes used in small sample statistics [Walpole and Myers, 1985], one can say that if $E_{max,syst}$ < 3×SEM it is unlikely (here: 5%) that the result can be improved by a second compensation. We put this rule-of-thumb to the test in Experiment #7, where $E_{max,syst}$ = 66 mm

was notably worse (the improvement over the uncompensated run was only 6.4-fold) than in the other experiments. Applying the above rule-of thumb, it is evident that 66 mm > 3×SEM = 33.6 mm, so that a second compensation run was indicated. After the second compensation, the vehicle's error was $E_{max,syst}$ = 20 mm, i.e., a 21-fold reduction relative to the uncompensated systematic error.

Table III: The *Measure of Dead-reckoning Accuracy for Systematic Errors*, $E_{max,syst}$, before and after compensation.

Experiment # and Fig.	$E_{max,syst}$ before compensation [mm]	$E_{max,syst}$ after compensation [mm]	Improvement	Comment
E-1	317	21	15-fold	Details also shown in Fig. 6.5
E-2	349	32	11-fold	
E-3	310	31	10-fold	These 3 experiments used the same set of uncalibrated results and identical correction factors.
E-4	310	14	22-fold	
E-5	310	26	12-fold	
E-6	403	35	11-fold	
E-7	423	after 1st comp: 66 after 2nd comp: 20	21-fold*	In this experiment the diameter of the right wheel was slightly increased by winding three loops of masking tape around the wheel perimeter.
E-8	232	12	19-fold	In this experiment the diameter of the left wheel was slightly increased by winding five loops of masking tape around the left wheel perimeter.

*) *Two compensation runs were performed. See explanation in main text.*